Retrieval of Temperature Profiles in Tropical Cyclones from Resampled Advanced Technology Microwave Sounder (ATMS) Observations

Fuzhong WENG[1,2],Wenyu LI[3], Hao HU[3] and Xiang Fang[4]

1. Nanjing University of Information Science and Technology
2. University of Chinese Academy of Sciences
3. CMA Earth System Modeling and Prediction Centre (CEMC)
4. CMA Department of Integrated Observations

CONTENT

Microwave Sounding Instruments

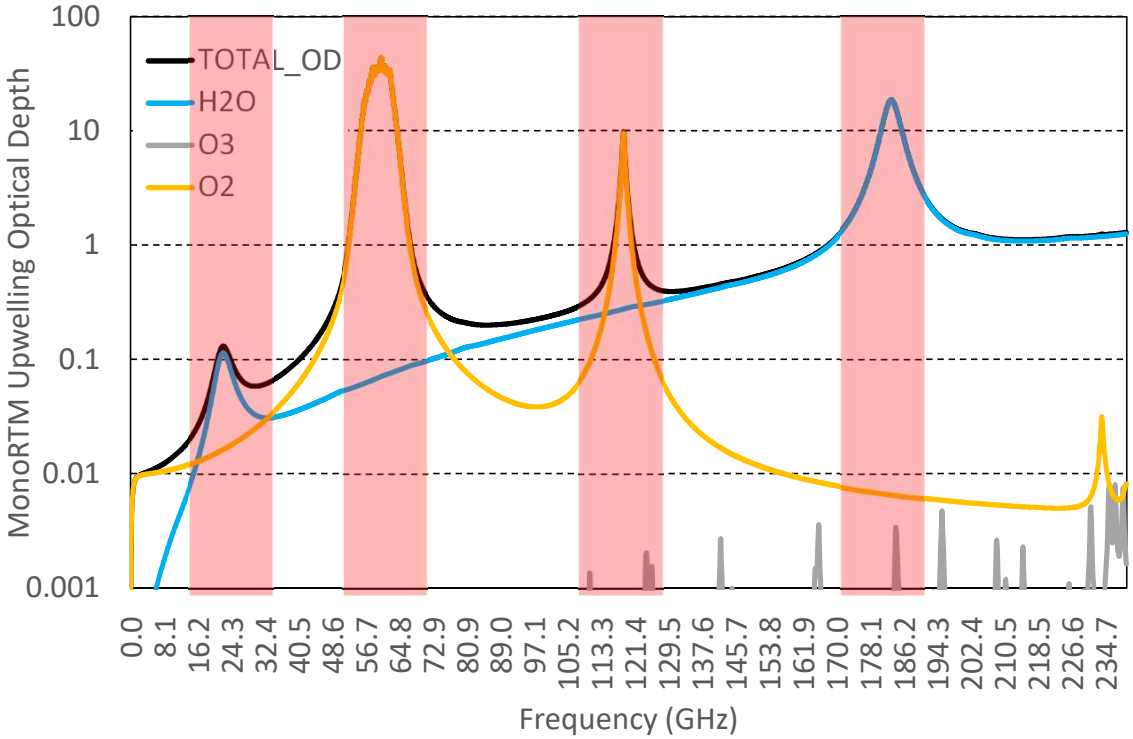

Three major absorption bands of MW sounding instruments:

LowO2: Low frequency oxygen absorption band (50-60 GHz)
HighO2: High frequency oxygen absorption band (118 GHz)
WV: Water vapor absorption band (183 GHz)

AMSU-A: LowO2
MHS: WV
SSMIS: LowO2+WV
ATMS: LowO2+WV
FY-3D/E MWTS+MWHS: LowO2+HighO2+WV

The foundation for retrieving instrument-agnostic products lies in utilizing similar channel combinations within the algorithm.

ATMS Scan Geometry and Its Influences

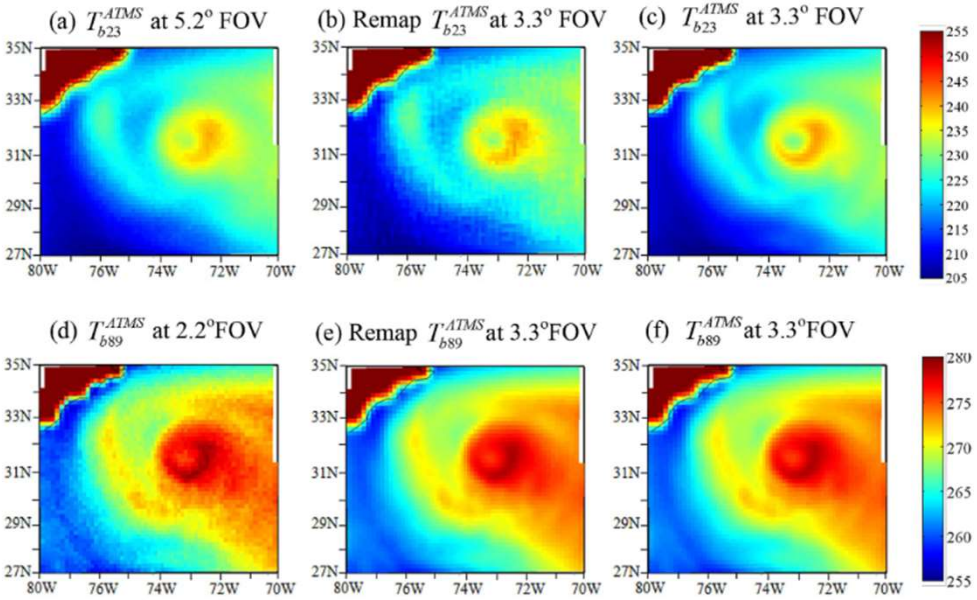

When using different beamwidth settings, the observations from different instruments may exhibit different characteristics and result in different structures from the same storms.

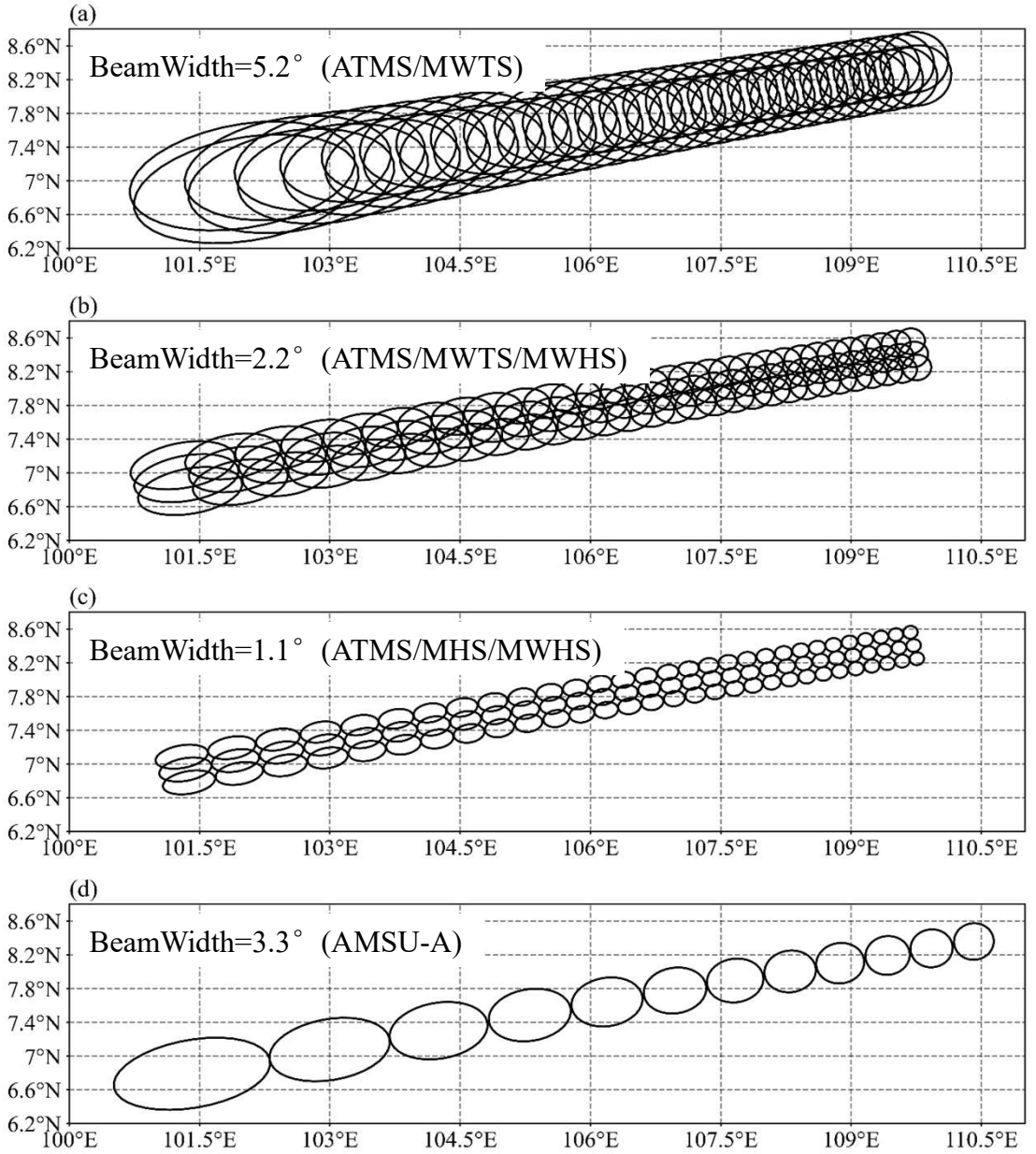

Monitoring Tropical Storm from Satellite Microwave Sounders

Microwave radiometers onboard satellites can receive the scattering and emitting radiation from clouds and precipitation and provide the data for detecting all-sky vertical thermal structures of **severe weather systems**.

Currently, microwave instruments are only available on polar-orbiting satellites. The **limited revisit time** significantly hinders their effectiveness in monitoring weather systems.

Multiple microwave sounding instruments from **different platforms** can significantly enhance the time resolution of microwave instrument products.

However, retrieved results often vary from different instruments due to their differences in spatial resolutions and channel configurations. **Thus, it is necessary to develop a retrieval system to produce instrument-agnostic products.**

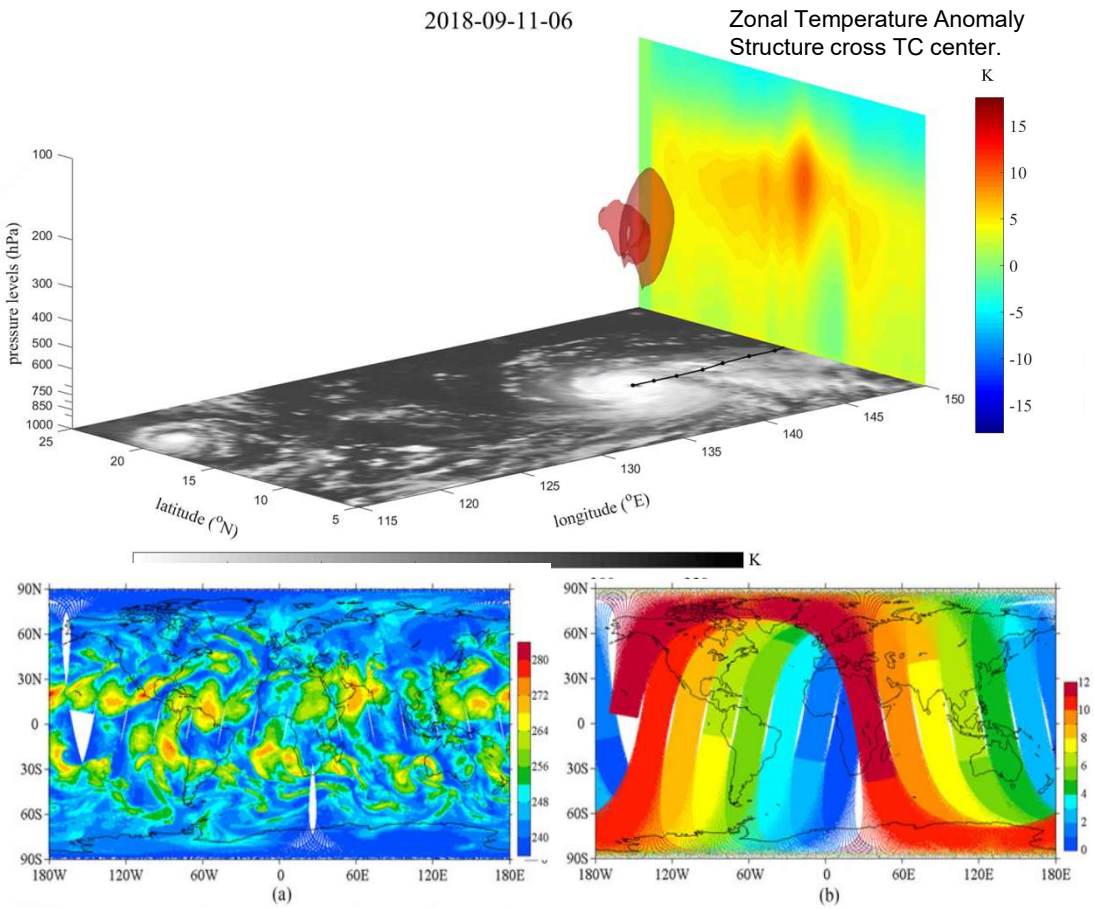

Ma et al. 2017

Atmospheric Temperature Derived from ATMS with Regression Algorithms

Many previous studies retrieved hurricane thermal structures from **regression-type algorithms**. But the retrieved results are sensitive to regression coefficients. It is very difficult to compare retrieval results from different algorithms and different instruments.

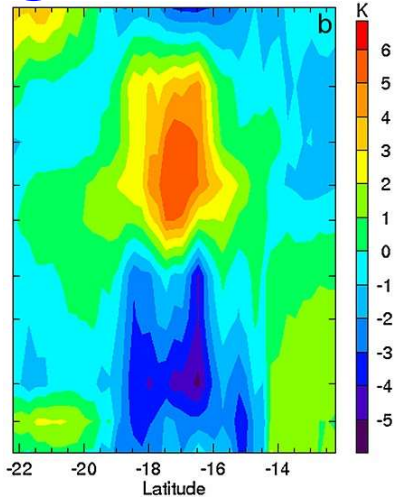

Zhu and Weng (2013)

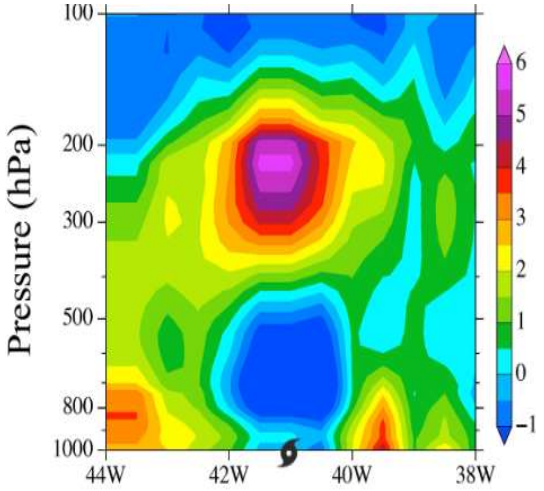

Tian and Zou (2016)

Recently, the **1DVAR retrieval method** has been developed (e.g. NOAA MiRS) for microwave sounders. 1DVAR performs variational iteration which takes into account instrument bias and observation errors

$$J(\mathbf{x}) = \frac{1}{2}(\mathbf{x}-\mathbf{x}_b)^T \mathbf{B}^{-1}(\mathbf{x}-\mathbf{x}_b) + \frac{1}{2}(H(\mathbf{x})-\mathbf{y}^{obs})^T(\mathbf{O}+\mathbf{F})^{-1}(H(\mathbf{x})-\mathbf{y}^{obs})$$

$$J(\mathbf{x}_a) = \min_{\mathbf{x}} J(\mathbf{x}) \quad \forall \mathbf{x} \text{ near } \mathbf{x}_b$$

- $\mathbf{x}$ – analysis variable
- $\mathbf{x}_a$ – final analysis
- $\mathbf{x}_b$ – background
- $\mathbf{B}$ – background error covariance
- $\mathbf{y}^{obs}$ – observations
- $\mathbf{O}$ – observation error covariance
- H – observation operator
- $\mathbf{F}$ – forward model error covariance

Global Scene-Dependent Atmospheric Retrieval Testbed (GSDART)

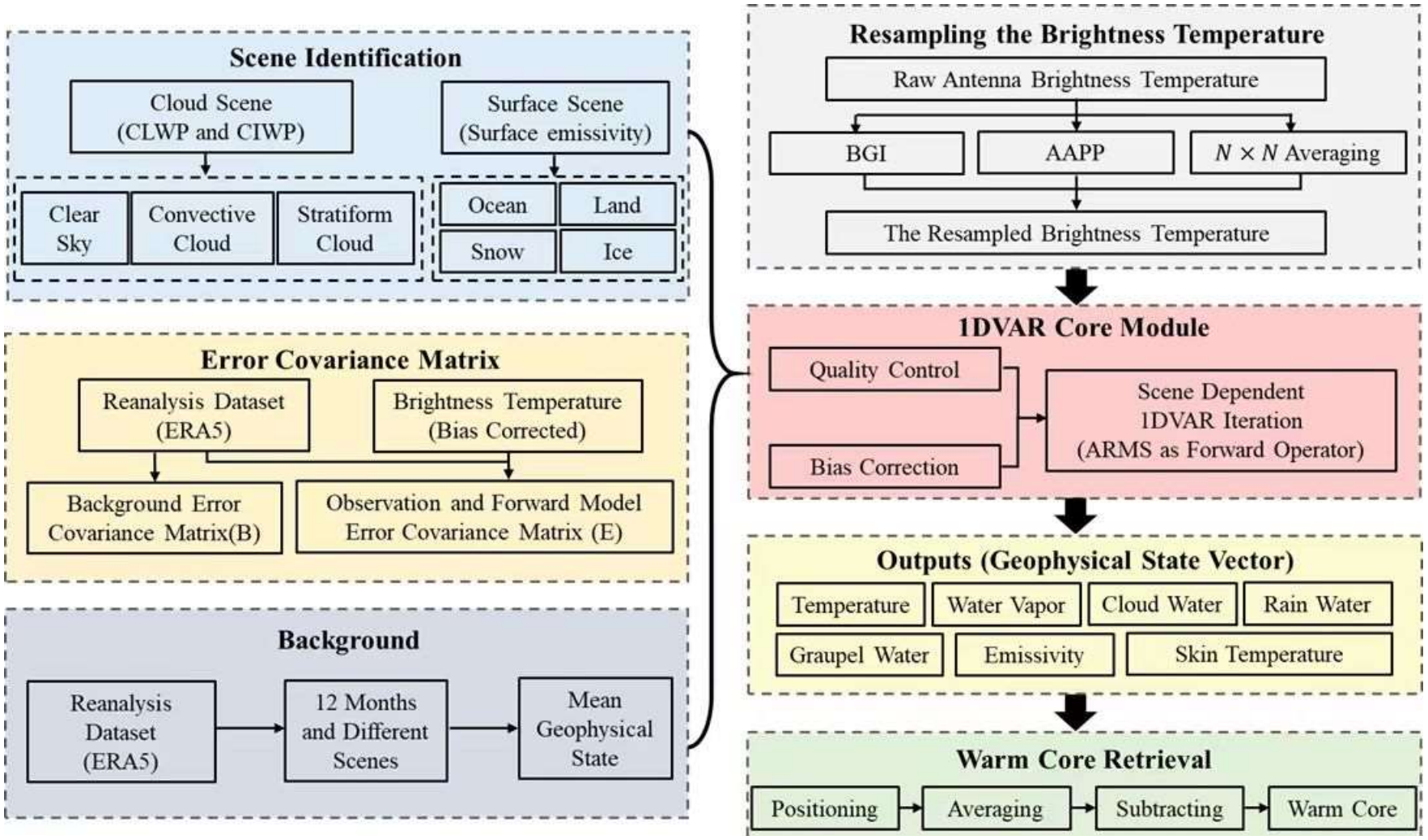

GSDART Physics

$$J(\mathbf{x}) = \frac{1}{2}(\mathbf{x}-\mathbf{x}_b)^T \mathbf{B}^{-1}(\mathbf{x}-\mathbf{x}_b) + \frac{1}{2}(H(\mathbf{x})-\mathbf{y}^{obs})^T(\mathbf{O}+\mathbf{F})^{-1}(H(\mathbf{x})-\mathbf{y}^{obs})$$

$$J(\mathbf{x}_a) = \min_{\mathbf{x}} J(\mathbf{x}) \quad \forall \mathbf{x} \text{ near } \mathbf{x}_b$$

- $\mathbf{x}$ – analysis variable
- $\mathbf{x}_a$ – final analysis
- $\mathbf{x}_b$ – background
- $\mathbf{B}$ – background error covariance
- $\mathbf{y}^{obs}$ – observations
- $\mathbf{O}$ – observation error covariance
- H – observation operator
- $\mathbf{F}$ – forward model error covariance

ARMS is used as a forward model. The scene-dependent **Xb** and **B** are generated.

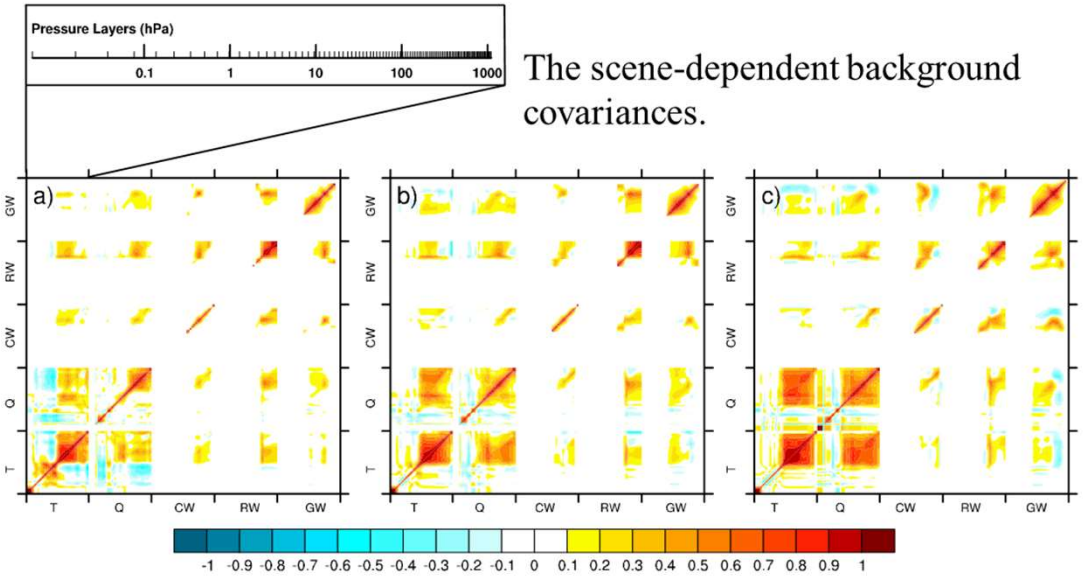

The scene-dependent background covariances.

Hydrometer **B** and **Xb** are generated based on WRF simulation.

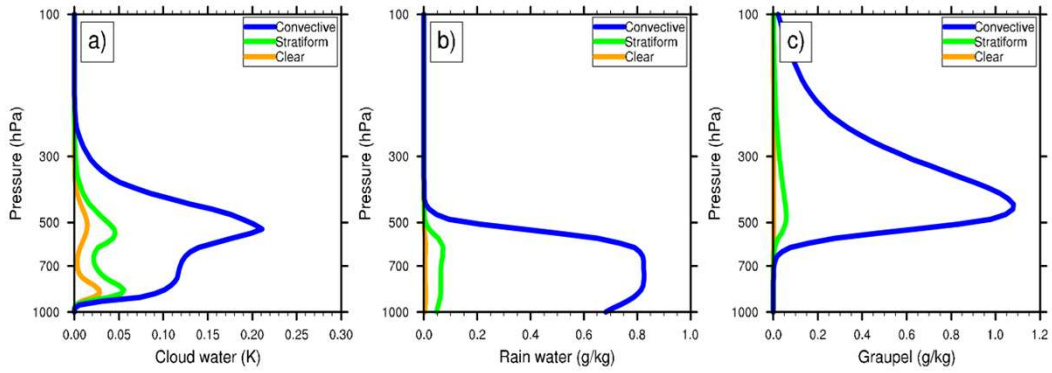

$$\begin{cases} mdbz > 39\ dBZ & convective \\ RainRate < 0.1\ mm/hr & clear \\ Others & stratiform \end{cases}$$

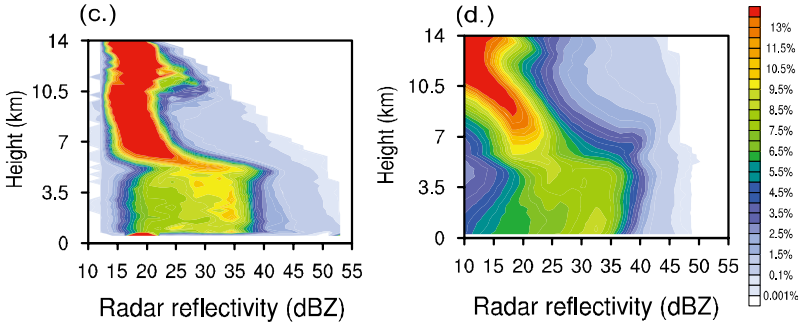

Evaluation of Temperature & Humidity Profile from GSDART

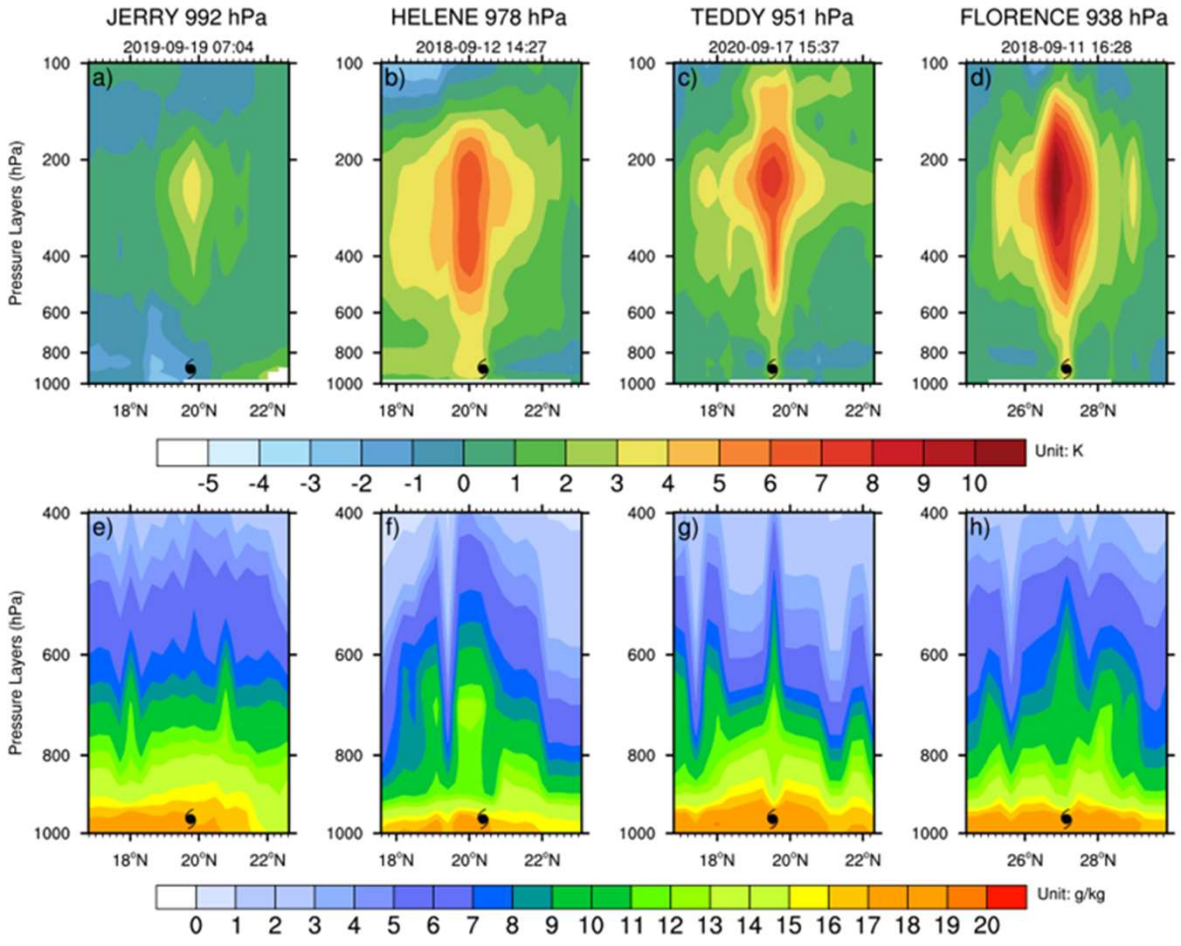

Hu and Weng 2022

Based on the scene-dependent covariance 1DVAR method, the warm core structure could be retrieved for any stage of TCs.

Compared with flight dropsonde observations under TC conditions, the temperature and humidity errors could be reduced to around 1.5 K and 10-20%, respectively, throughout the troposphere.

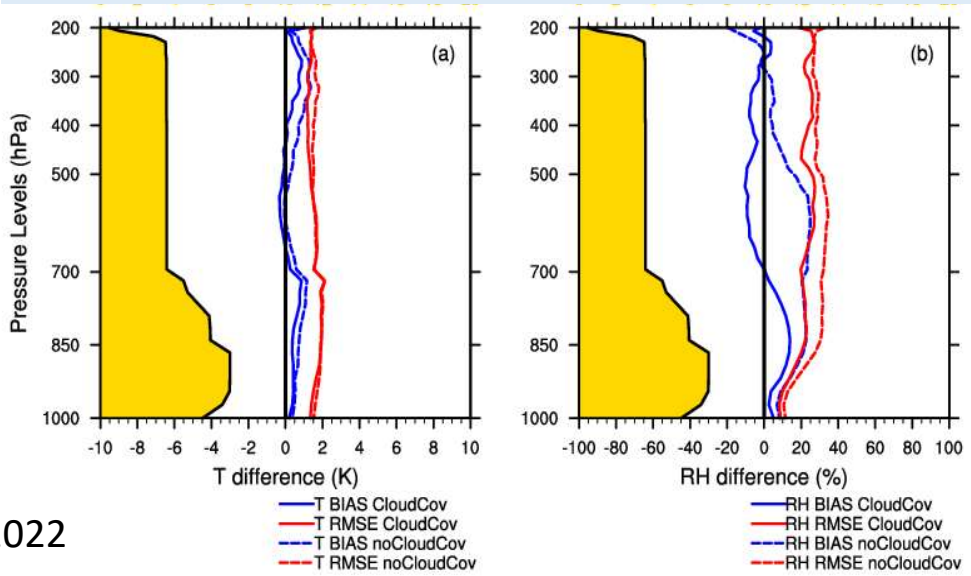

Resampling ATMS Data

Microwave Sounding Data from MSU to AMSU/MHS to ATMS

ATMS Field of View Size for the beam width of 2.2° – black line

ATMS Resample to the Field of View Size for the beam width of 3.3°- blue line

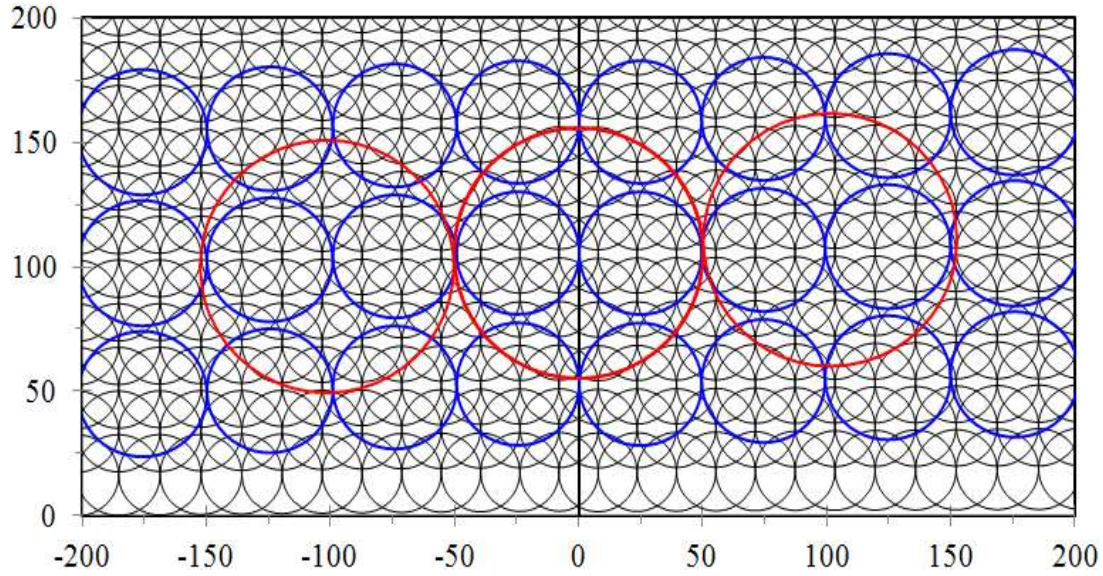

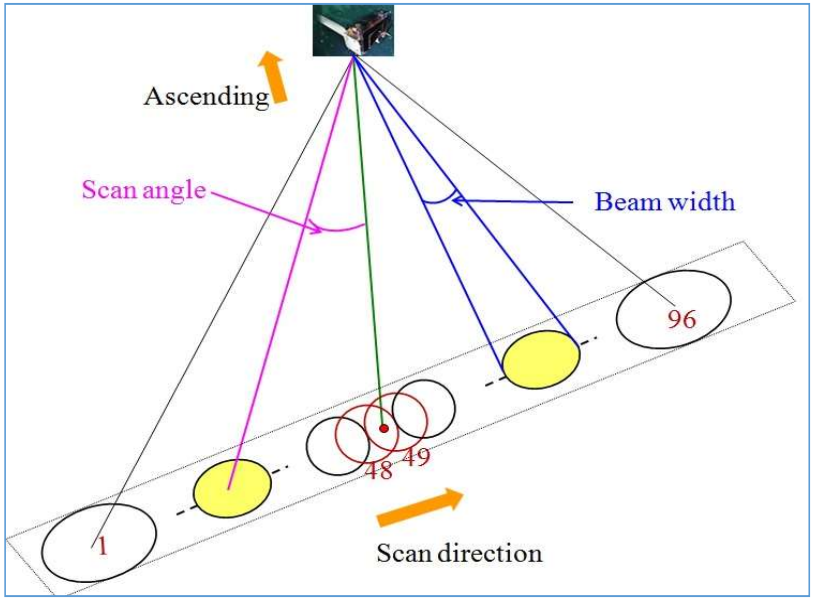

Noise Reduction from Resampling

ATMS Channels 3-16

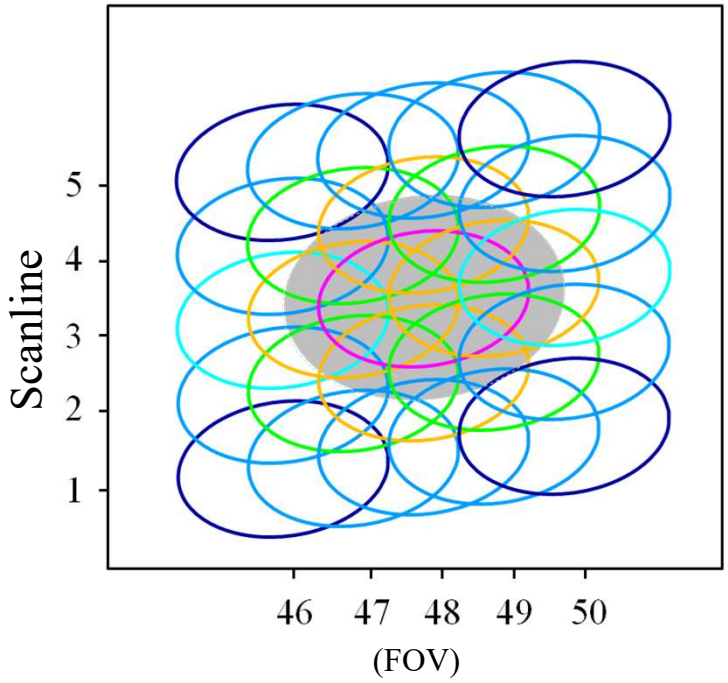

ATMS Channels 1-2

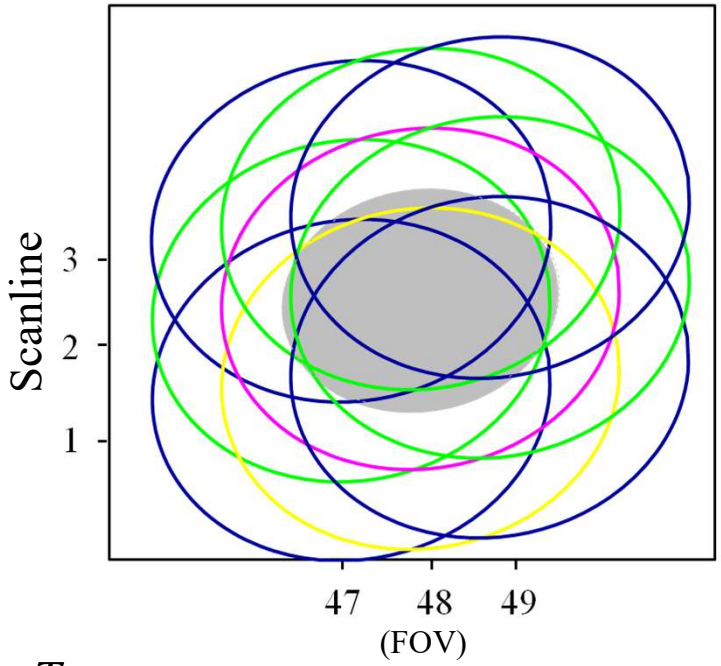

Noise for single observation

$$NE\Delta T = \frac{T_{sys}}{\sqrt{B \cdot \tau}}$$

Noise after average over multiple (9) looks

$$NE\Delta T = \frac{T_{sys}}{3 \cdot \sqrt{B \cdot \tau}}$$

Comparison of Resampling Algorithms

Modified AVHRR and ATOV Processing Package (AAPP)

$$\mathrm{MTF}(f,w) = \exp\left(-\frac{(\pi f w/2)^2}{\ln 2}\right)$$

$$\mathrm{T}_a^{target} = \mathrm{T}_a^{source} \times \frac{\mathrm{MTF}(f^{target}, w^{target})^{target}}{\mathrm{MTF}(f^{source}, w^{source})^{source}}$$

$$\frac{\mathrm{MTF}(f^{target}, w^{target})^{target}}{\mathrm{MTF}(f^{source}, w^{source})^{source}} \times \exp\left(-\frac{(\ln \mathrm{MTF}(f^{target}, w^{target})^{target})^2}{(\ln c)^2} \ln 2\right)$$

BGI- Buckus Gilbert Inversion

$$T_b^{BG}(k) = \sum_{i=-N_{ch}}^{N_{ch}} \sum_{j=-N_{ch}}^{N_{ch}} w(k+i,j) T_b^{ATMS}(k+i,j)$$

$w(k+i,j)$ – B-G coefficients

$$N_{ch} = \begin{cases} 1 & \text{Channels 1-2} \\ 2 & \text{Channels 3-16} \end{cases}$$

3*3 Avg.

Specifically, excluding the FOVs on both sides of the scanning track and the two FOVs at the top and bottom of the image, the 3×3 FOVs averaging algorithm involves averaging the values of each target FOV with its surrounding 3×3 FOVs. This means that 8 FOVs adjacent to the target FOV are selected and their original values are averaged to generate a new value of the target FOV.

Influence of Resampling Algorithm on ATMS Channel 1 at 23.8 GHz

- The data resampled using 3×3 FOVs averaging algorithm is closer to the original brightness temperature compared to the other two algorithms.
- BGI and AAPP tend to have significant errors in the areas surrounding clouds and land/coast regions.
- Main discrepancies between BGI and AAPP also occur in the regions surrounding clouds and land/coast areas.

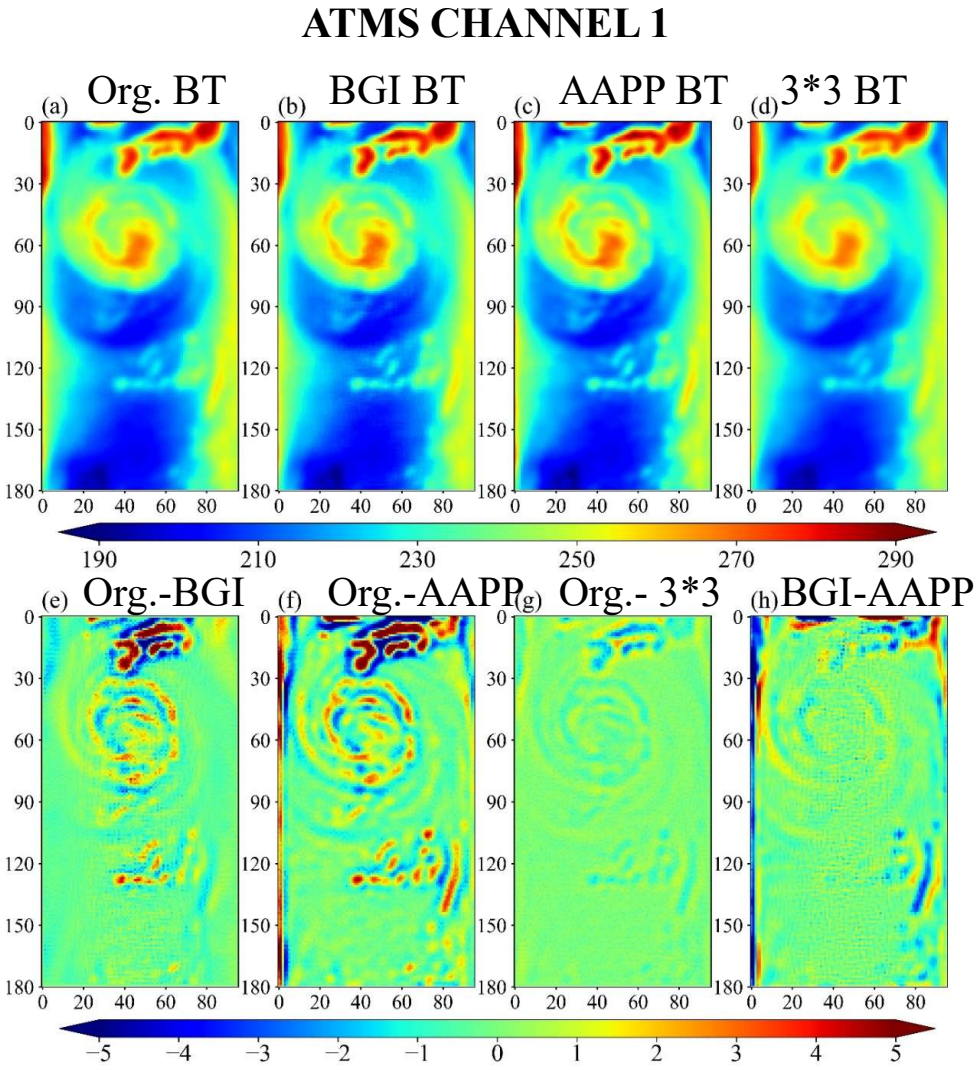

Influence on ATMS Upper Air Sounding Channels

ATMS CHANNEL 15

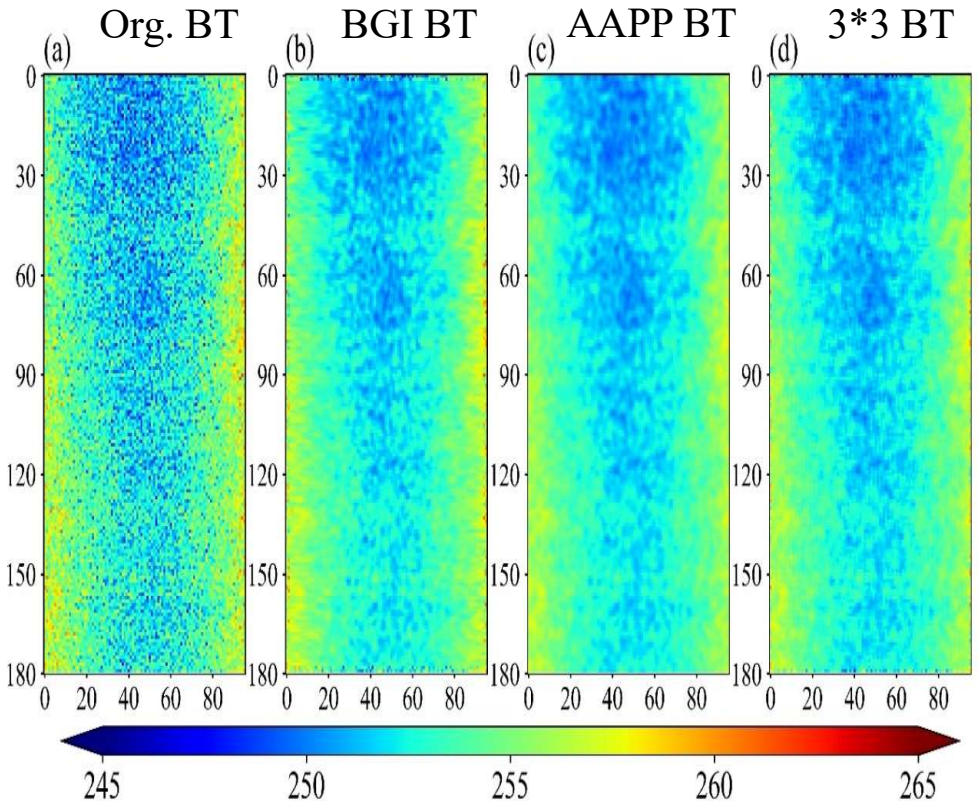

- After resampling the data, there was a noticeable decrease in noise in the upper-level sounding channels from 13-15.
- The BGI, AAPP, and 3x3 FOVs averaging algorithms all have effects on resolution.
- BGI and AAPP algorithms exhibited superior noise reduction, compared to the 3×3 FOVs averaging algorithm.

Influence on Retrieved Warm Cores

ATMS retrieved warm core of Nanmadol

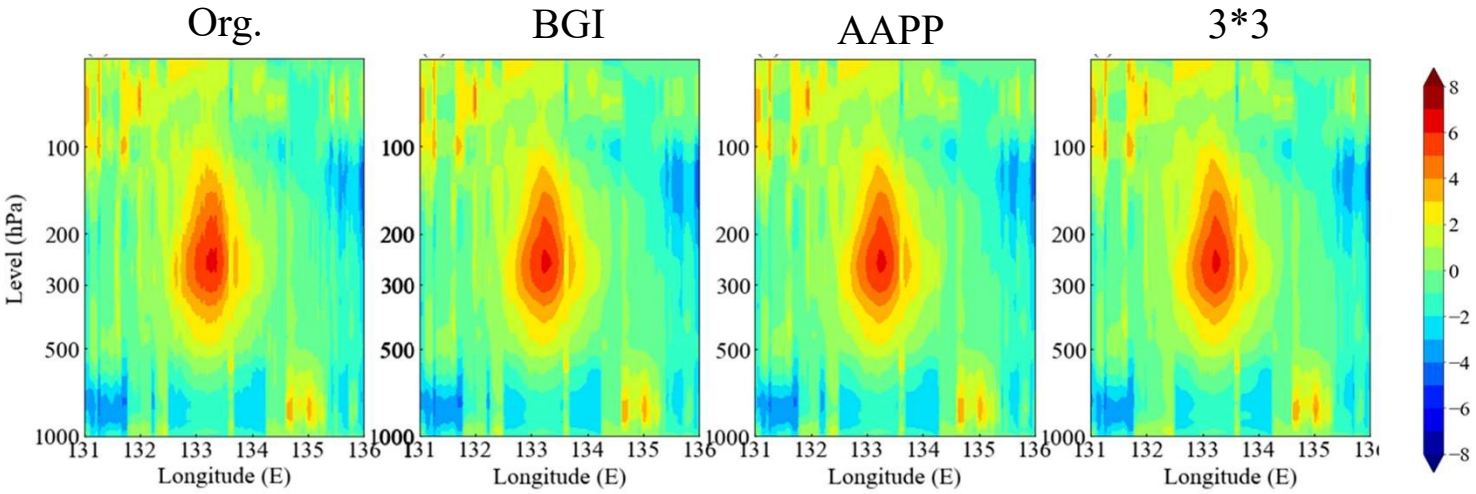

ATMS retrieved Temp. anomaly @ 250 hPa of Nanmadol

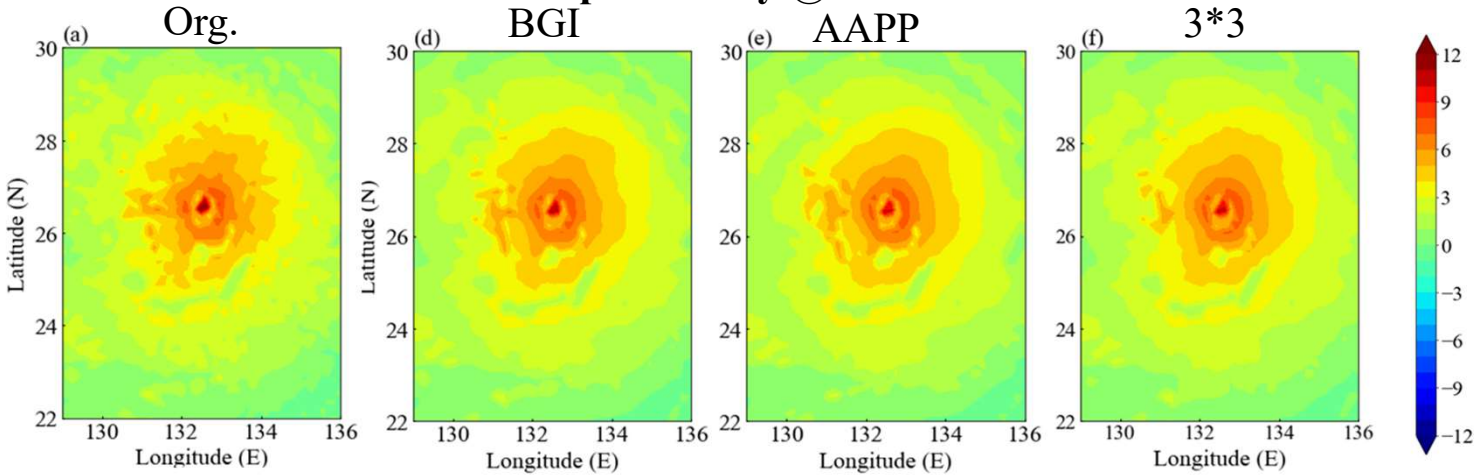

By resampling, the noise can be greatly reduced, leading to a better convergence rate and retrieval speed when using the 1DVAR algorithm. This results in a nice warm warm core structure and less anomalous fluctuations around the storm.

However, reducing the resolution can significantly affect the warm core intensity in the center of the tropical cyclone, causing a decrease of around 2K.

Applications of GSDART to FY-3 Combined Sounding Data Stream

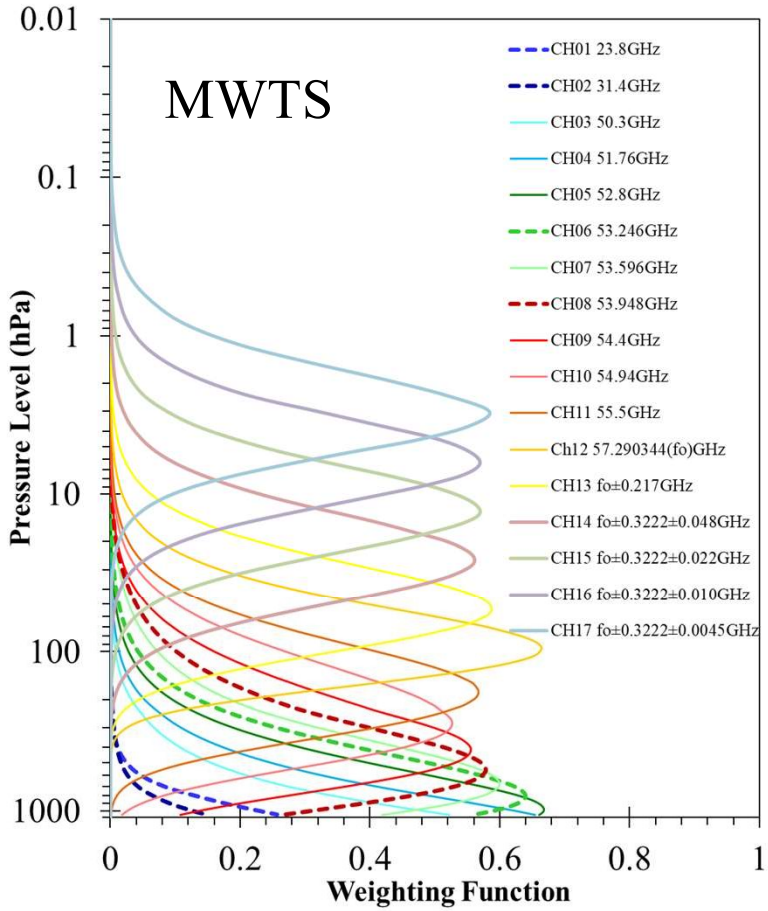

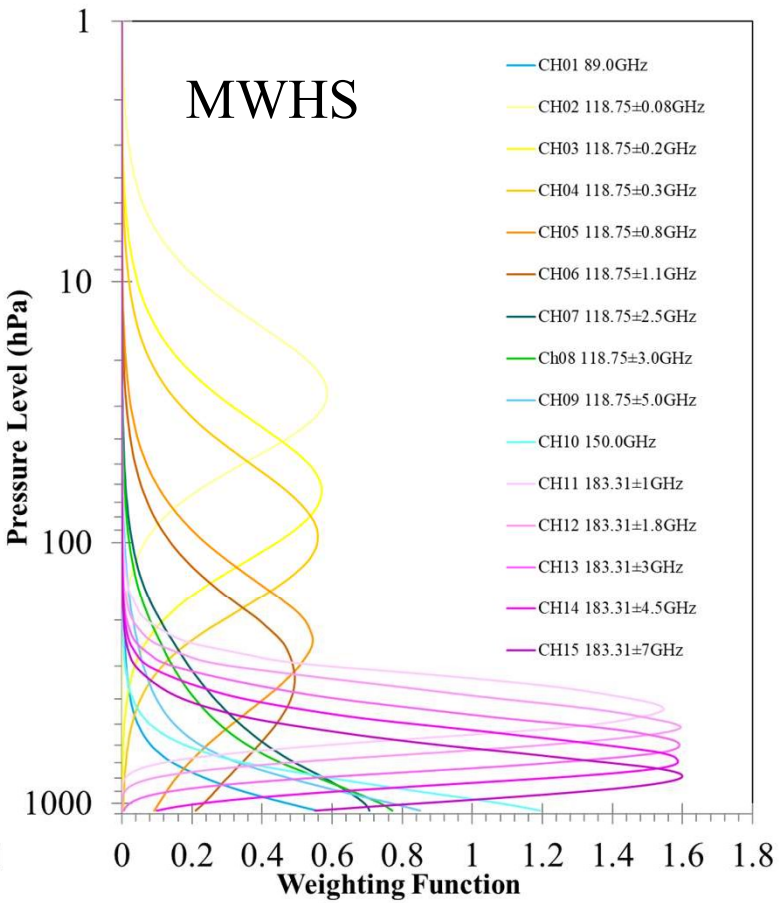

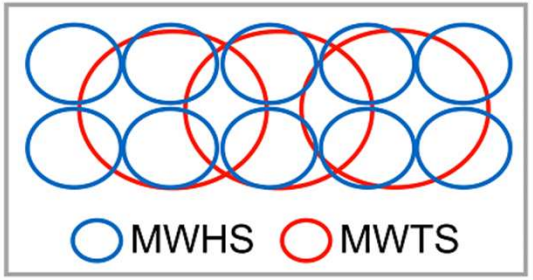

To guarantee **uniform channel configuration** among various instruments and enable them to obtain 3D temperature and water vapor products together, we utilize the ATMS instrument's channel configuration as a reference to align and merge temperature and humidity sensors from other sources.

Comparison of ATMS and CMWS Weighting Functions

NOAA ATMS (22 Channels)

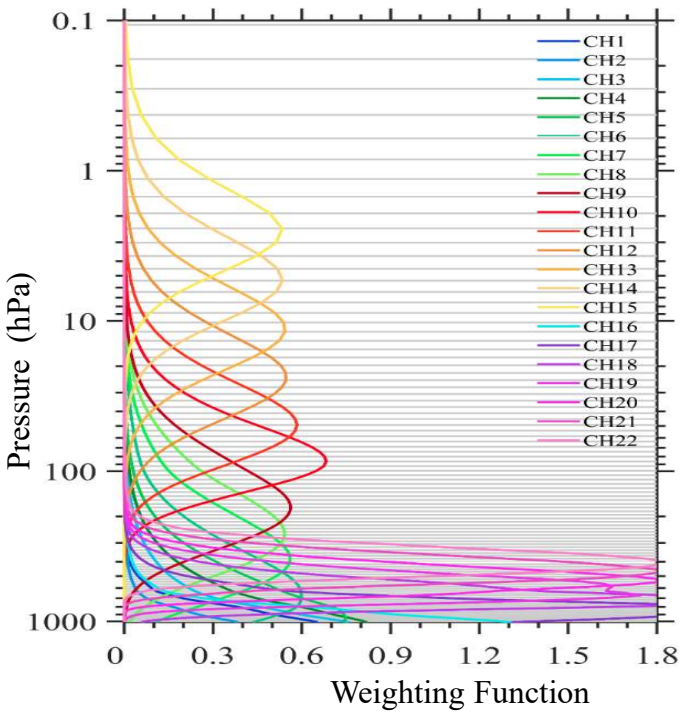

CMA CMWS (32 channels)

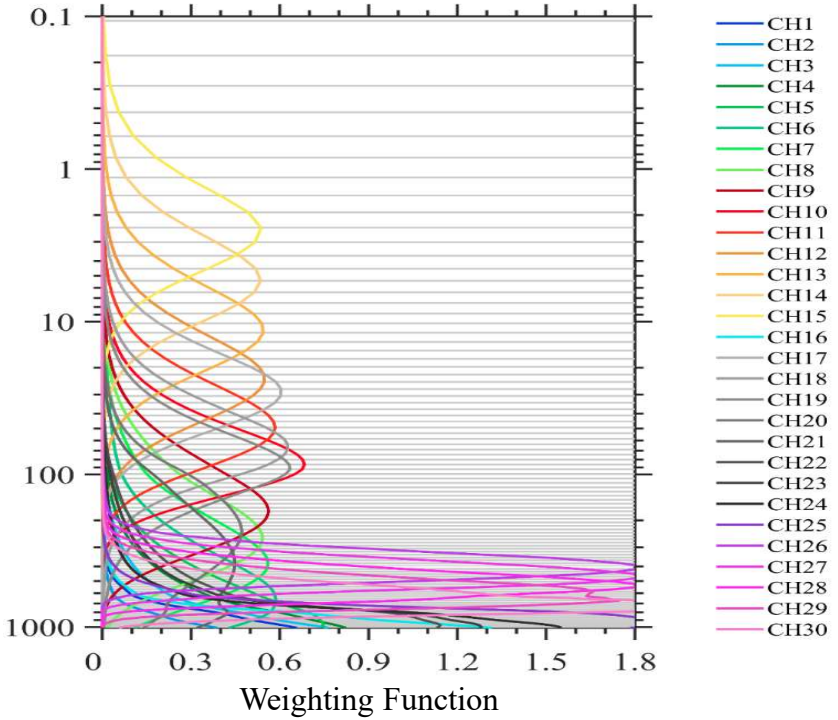

Combined MicroWave sounding Suite (CMWS) from FY-3E MWTS and MWHS has a better vertical resolution for atmospheric sounding than NOAA ATMS

Comparison of Thermal Structures Derived from ATMS and CMWS

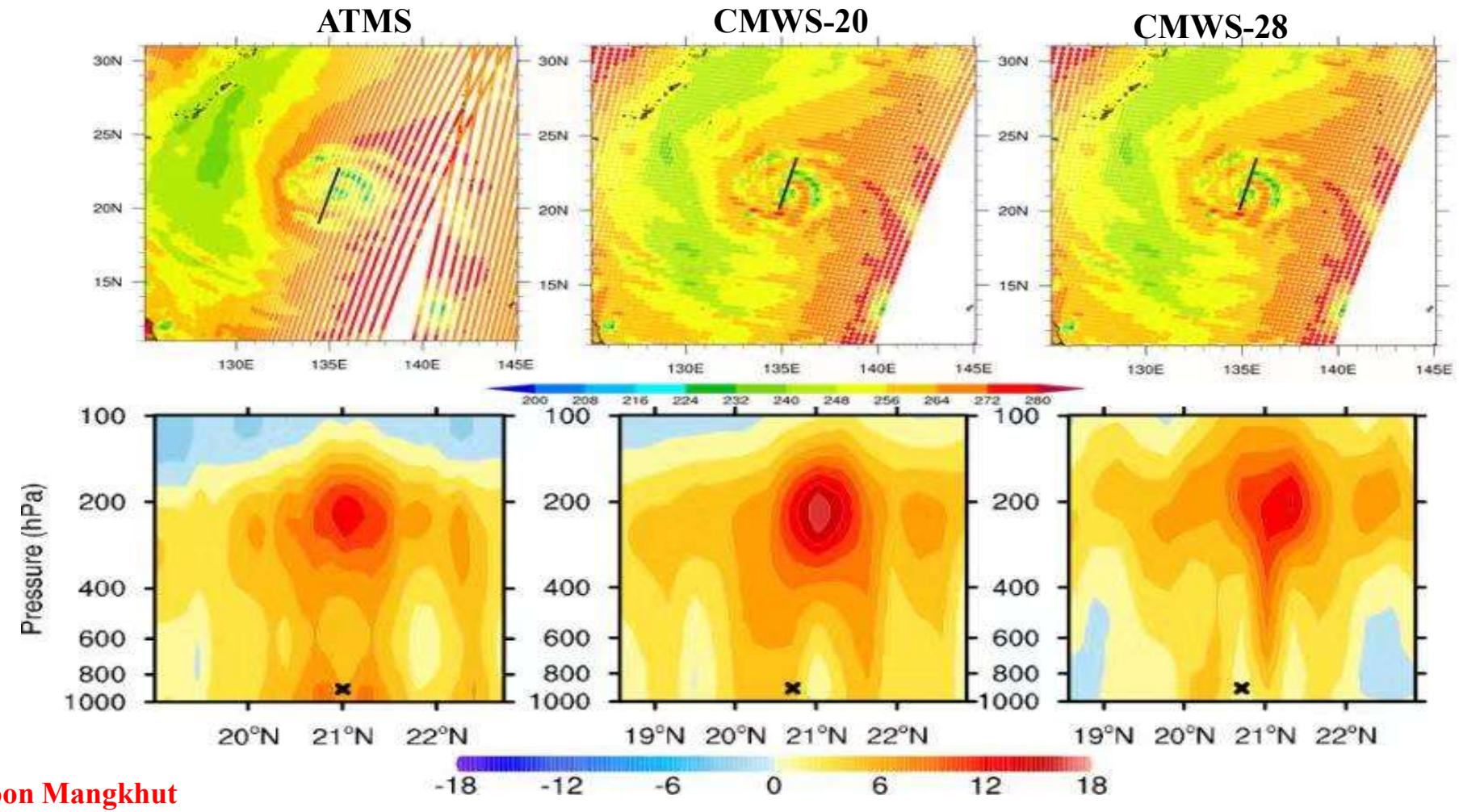

Typhoon Mangkhut

FY-3 CWMS Warm Core Evaluations

Typhoon Mangkhut

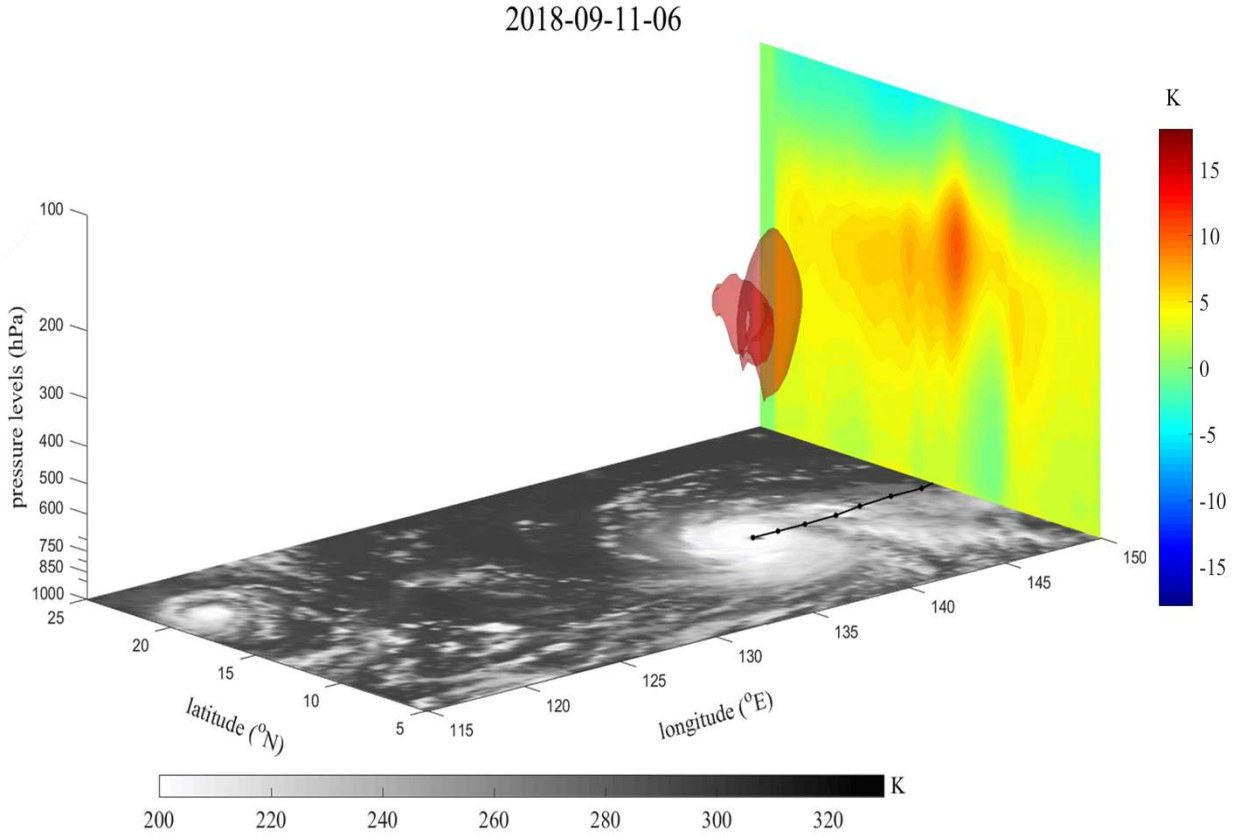

Assessments on FY-3 Retrieved Temperature and Humidity Profiles

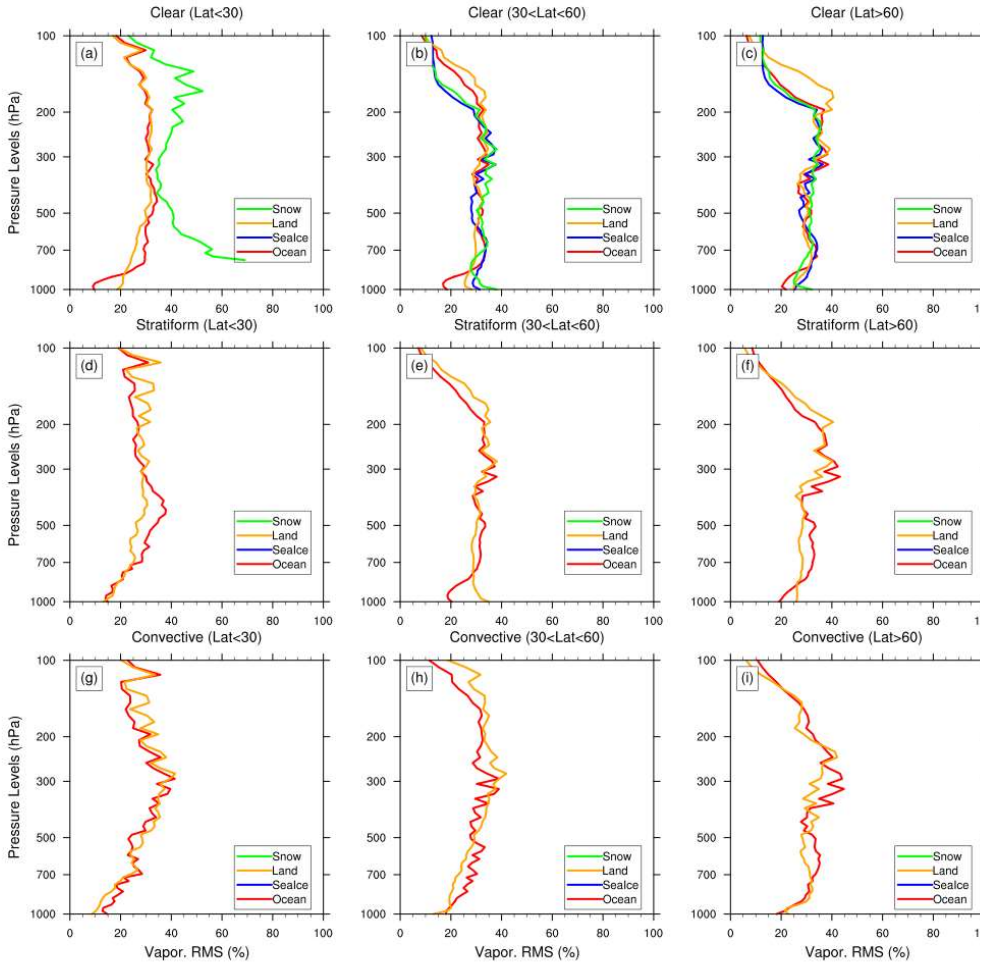

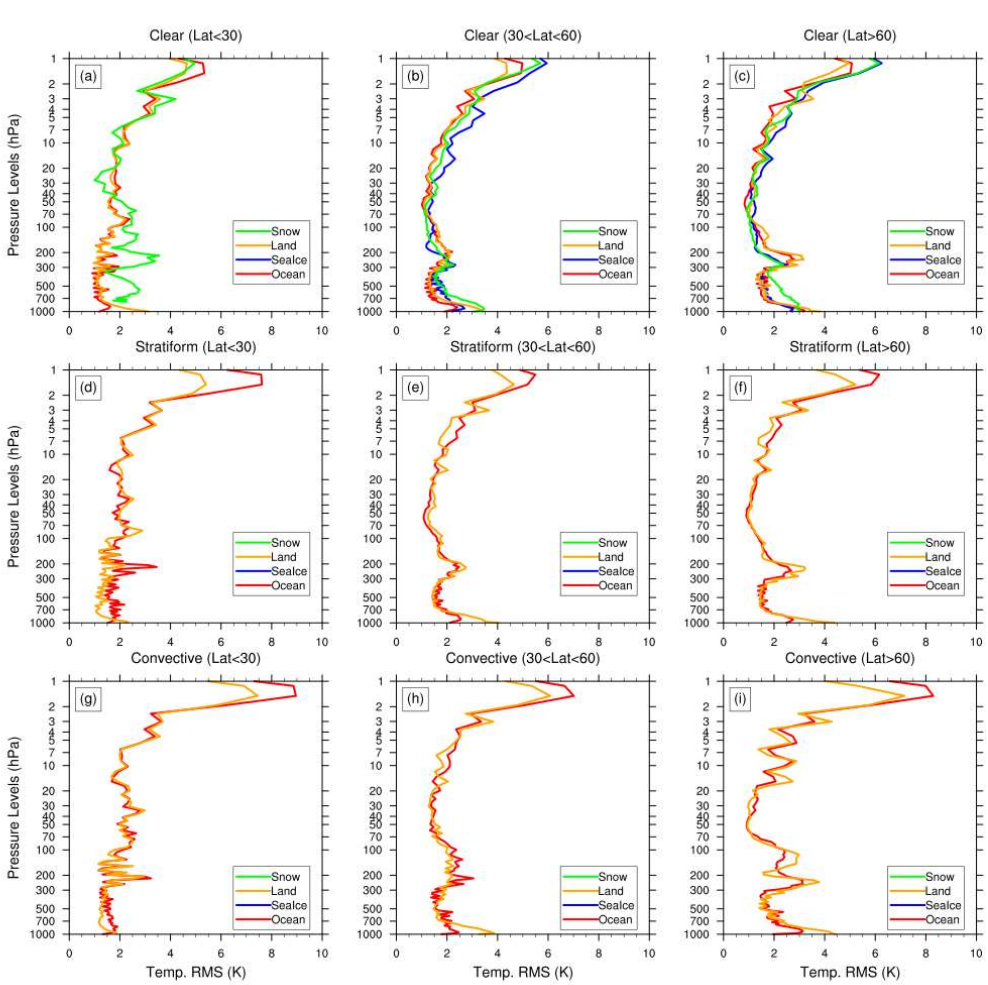

Comparison of Thermal Structures Derived from ATMS and CMWS with Different Algorithms

CMWS vs ATMS

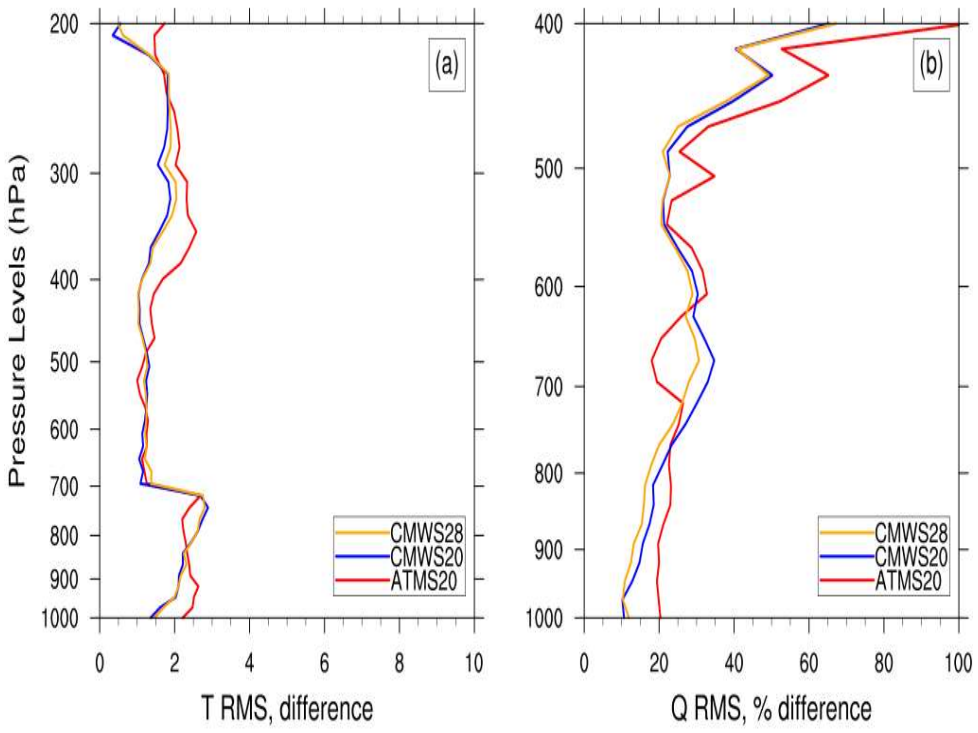

MIRS vs GSDART

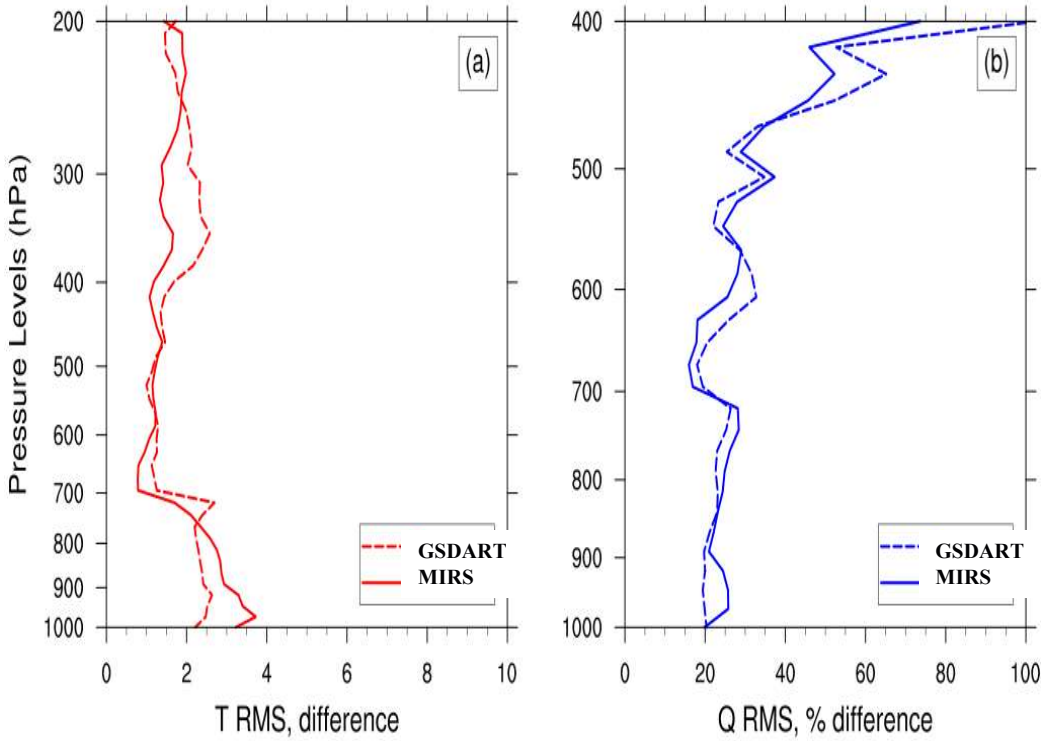

CMWS has a better performance than ATMS

GSDART has a better performance than MIRS

Surface Pressures Derived from Microwave Sounders

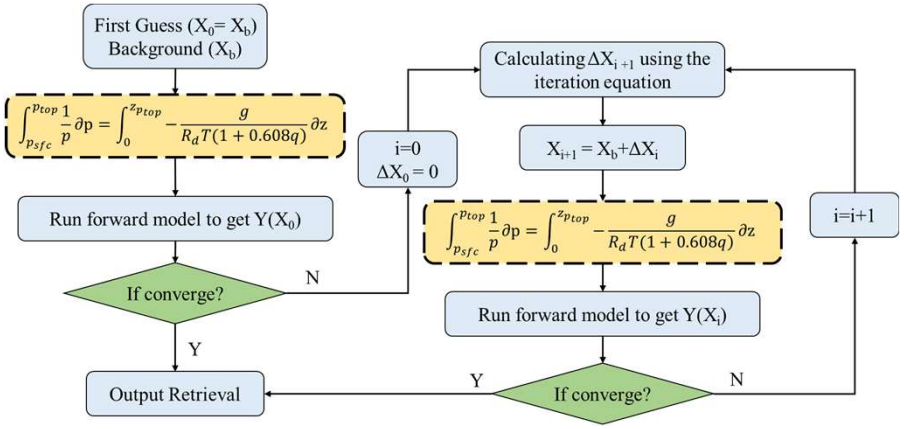

EXP. NAME	Description
EXP_ctrl	Psfc directly retrieved based on background covariance.
EXP_hs	Psfc retrieved based on 1DVAR iteration coupled with hydrostatic balance.

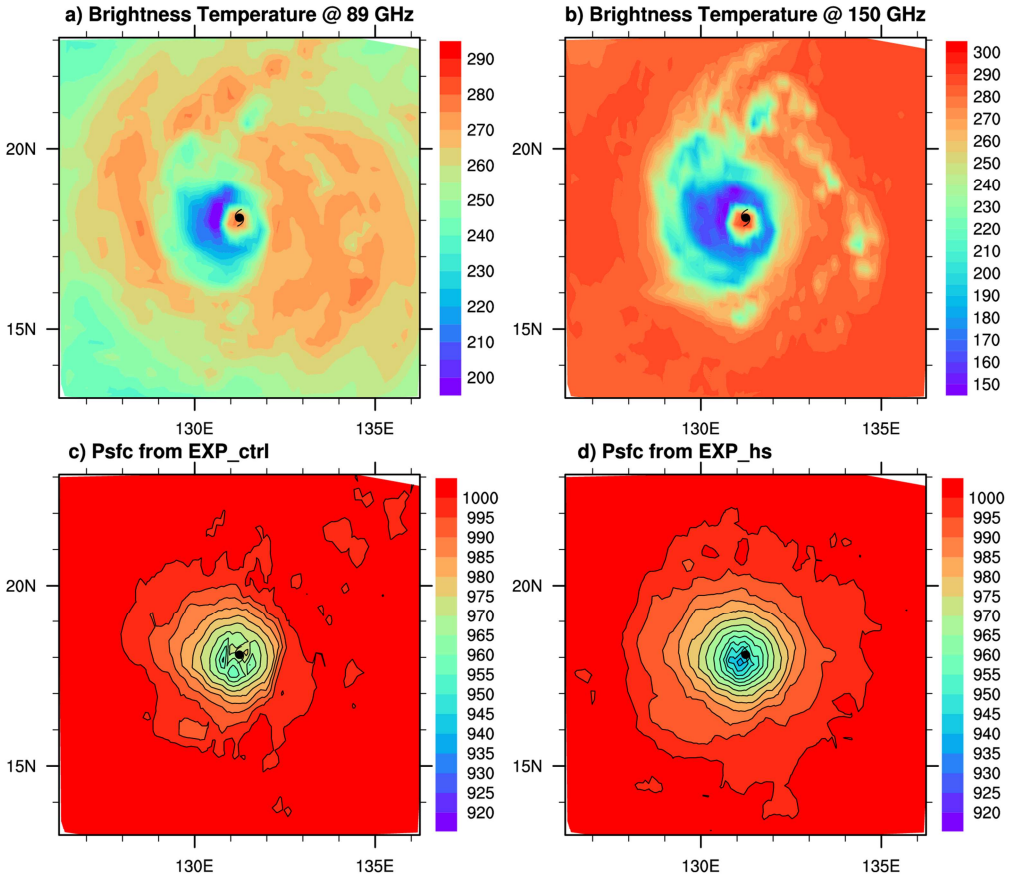

Surface Pressure Validated from Dropsonding Data

EXP. NAME	Description
EXP_ctrl	Psfc directly retrieved based on background covariance.
EXP_hs	Psfc retrieved based on GSDART iteration coupled with hydrostatic balance.

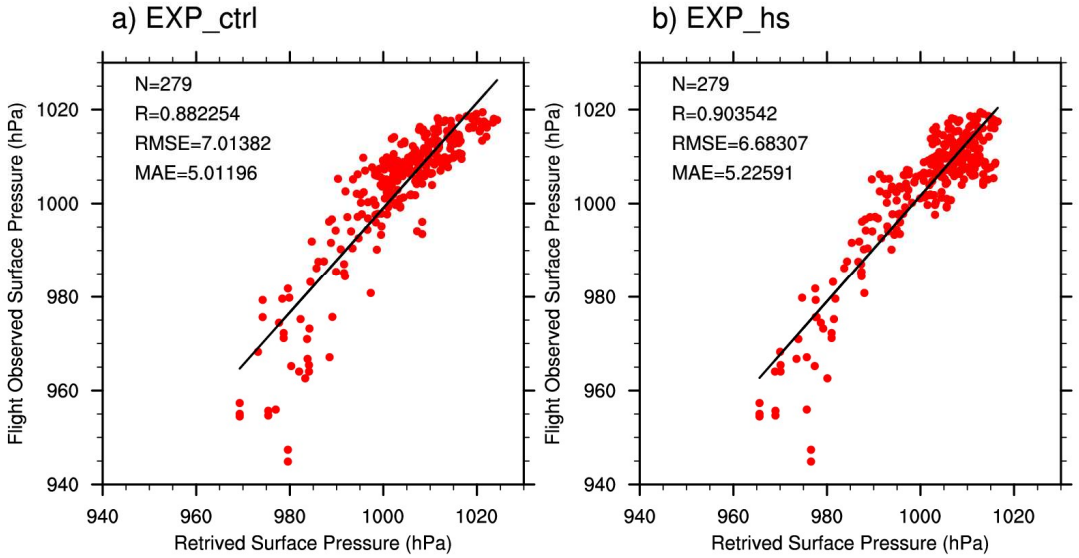

2018-2019: Atlantic and East Pacific aircraft dropsonding data

Pressure RMSE:6.68 hPa。

Retrieved Precipitation

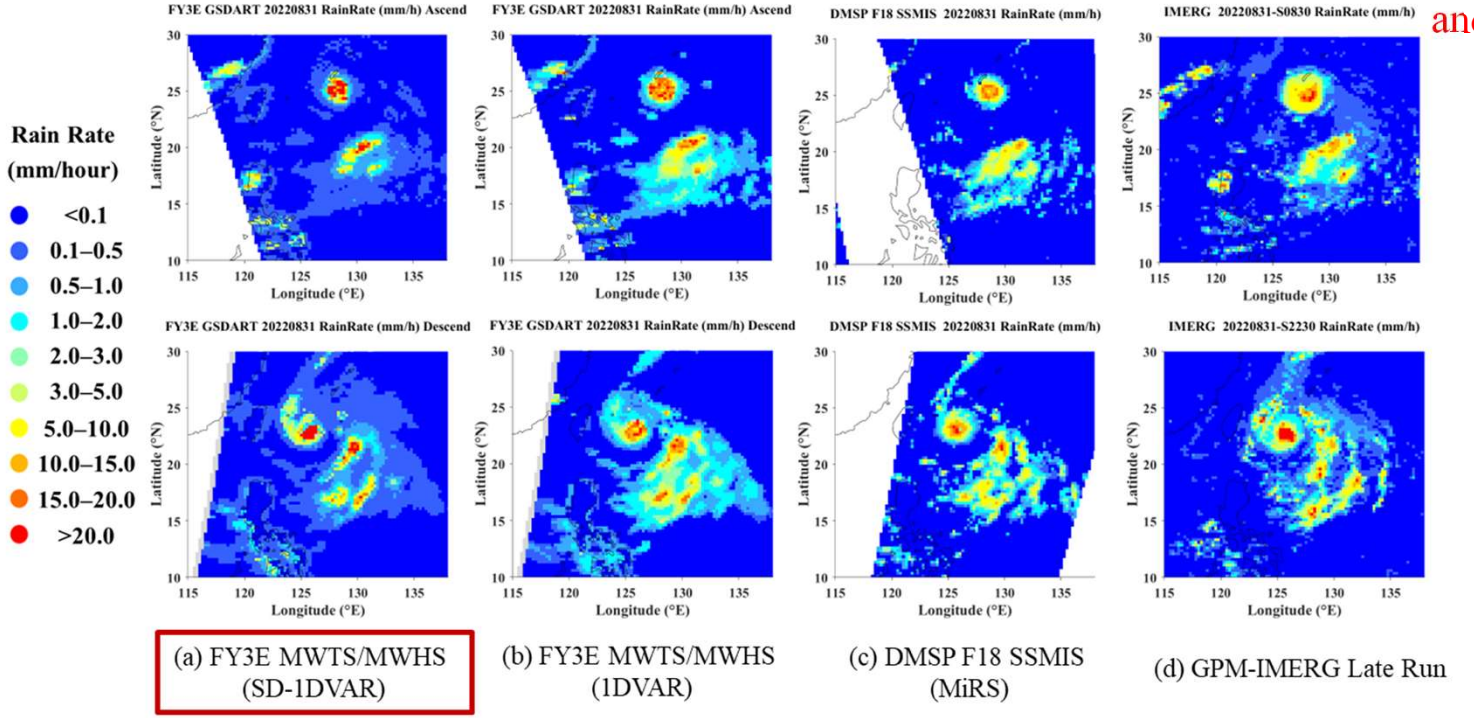

(a) FY3E MWTS/MWHS (SD-1DVAR)

(b) FY3E MWTS/MWHS (1DVAR)

(c) DMSP F18 SSMIS (MiRS)

(d) GPM-IMERG Late Run

Spatial distributions of precipitation rates for (a) FY3E MWTS/MWHS, (b) FY3E MWTS/MWHS (1DVAR), (c) DMSP F18 SSMIS (MiRS), and (d) GPM-IMERG LateRun on August 31, 2022. The first row is for ascending passes (~08:30 UTC), and the second row is for descending passes (~22:30 UTC).

Similar with FY-3D, precipitation product from GSDART performs better in capturing the light and heavy precipitation.

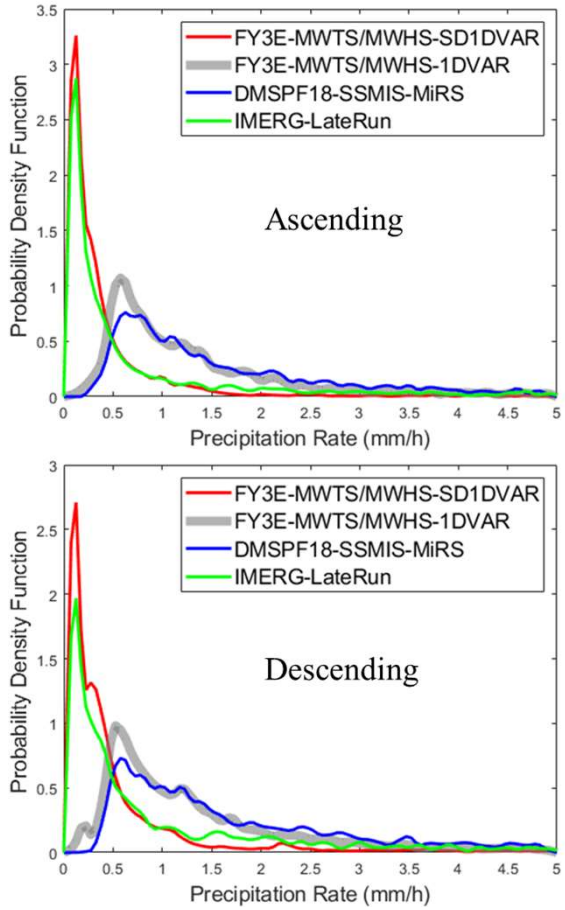

Typhoon Precipitation from FY-3 CMWS and Comparison with NOAA CMORPH

Precipitation from CMWS-28

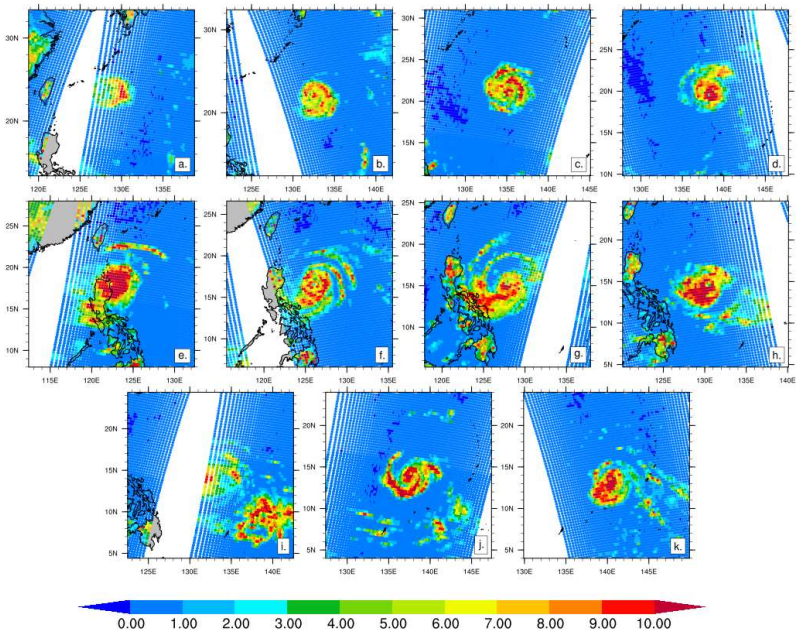

Precipitation from CMORPH

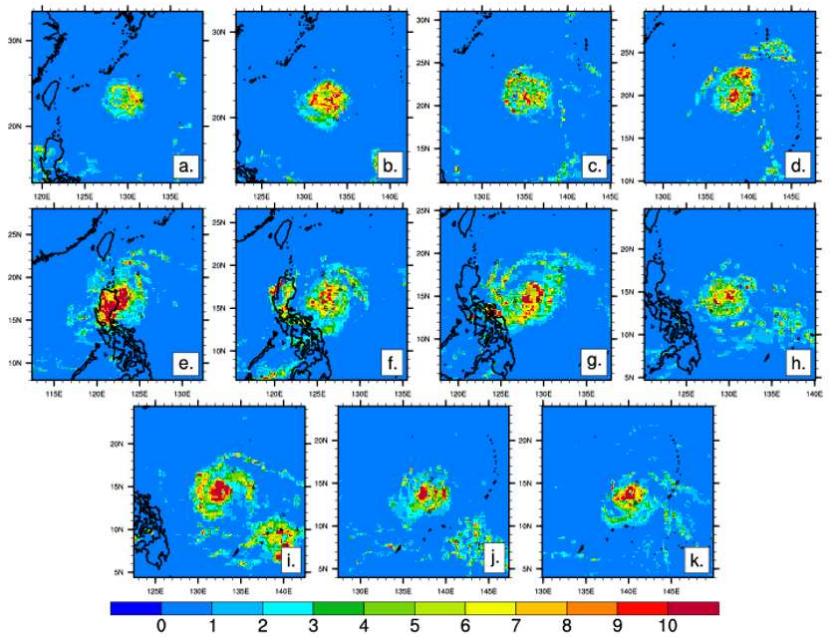

CMWS-28 is combined from MWTS and MWHS
CMORPH is NOAA multisensor precipitation products.

Cloud Liquid Water Distribution from FY-3 CMWS and NOAA ATMS

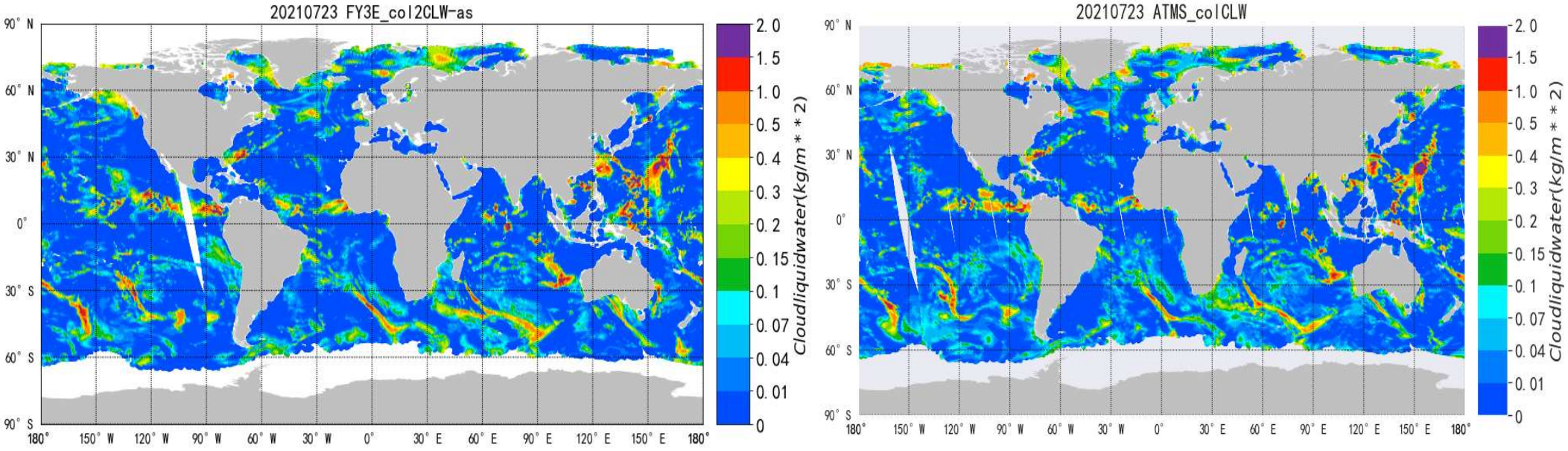

Both instruments can depict cloud liquid water very well. FY-3 has a larger scan swath and offer more spatial coverage

Monitoring Atmospheric River from FengYun/NOAA/METOP Microwave Sounding Systems

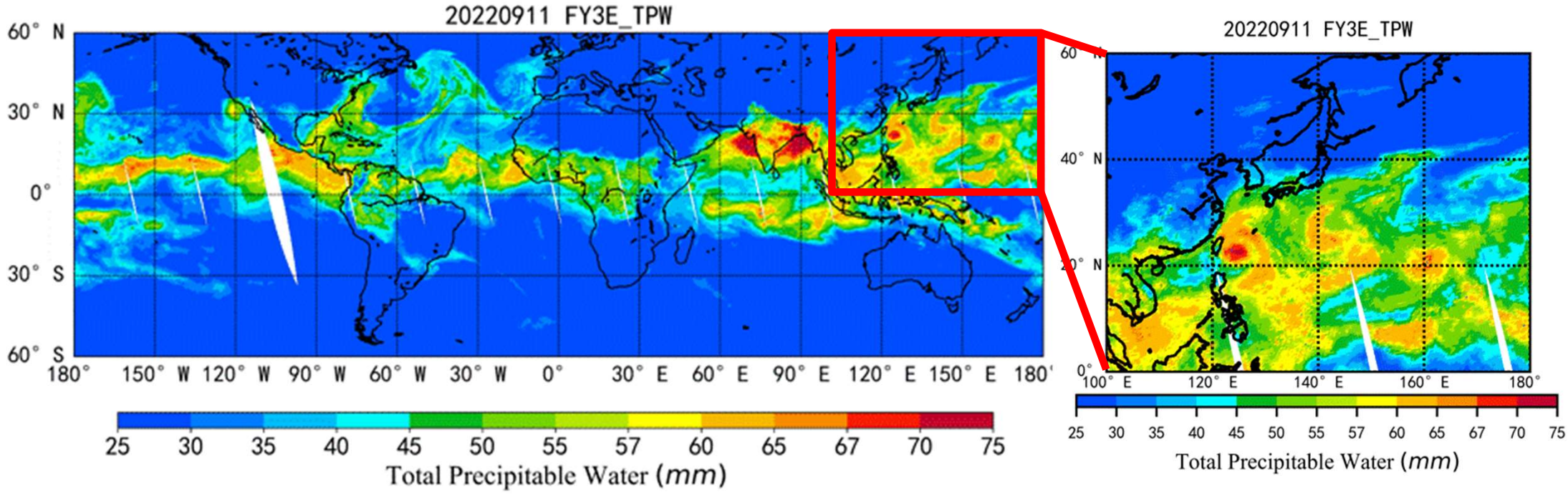

A constellation from FY/NOAA/METOC satellites allows for a high-frequency observations of atmospheric river evolution

Summary and Conclusions

- For creating instrument agnostic atmospheric parameters, it is important to use similar channel combination in the retrieval algorithms.
- Global scene dependent atmospheric retrieval testbed (GSDART) is developed and better suited for all the microwave sounding systems.
- Different resampling algorithms were tested for ATMS noise reduction. It is found that the BGI and AAPP algorithms are better for reducing the noise, compared to the 3x3 field-of-view averaging algorithm.
- A combination of FY-3 MWTS/MWHS offers much better sounding products in tropical cyclone system, compared to ATMS.